IEEE Access
Multidisciplinary | Rapid Review | Open Access Journal

Received August 3, 2019, accepted August 29, 2019, date of publication September 3, 2019, date of current version September 27, 2019.

Digital Object Identifier 10.1109/ACCESS.2019.2939151

Combining Proximity Estimation With Visible Symbol Assignment to Simplify Line-of-Sight Connections in Mobile Industrial Human-Machine Interaction

ZHEZHUANG XU[1,2], (Member, IEEE), ANGUO LIU[1], XI YUE[1], YULONG ZHANG[1], RONGKAI WANG[3], (Student Member, IEEE), JIE HUANG[1,2], (Member, IEEE), AND SHIH-HAU FANG[4], (Senior Member, IEEE)

[1]School of Electrical Engineering and Automation, Fuzhou University, Fuzhou 350000, China
[2]Key Laboratory of Industrial Automation Control Technology and Information Processing, Education Department of Fujian Province, Fuzhou 350000, China
[3]College of Control Science and Engineering, Zhejiang University, Hangzhou 310027, China
[4]Department of Electrical Engineering, Yuan Ze University, Taoyuan 320, Taiwan

Corresponding author: Jie Huang (jie.huang@fzu.edu.cn)

This work was supported in part by the NSF of China under Grant 61973085, Grant 61673116, and Grant 61703106, in part by the National Key Research and Development Program of China under Grant 2018YFB1702100, in part by the NSF of Fujian Province of China under Grant 2018J01790 and Grant 2017J01500, and in part by the Ministry of Science and Technology, Taiwan under Grant MOST 108-2634-F-155-001.

ABSTRACT The mobile industrial human-machine interaction plays an important role in the industrial internet of things, since the engineers can use a mobile device to interact with machines that greatly improves the efficiency and safety. Nevertheless, connecting to a specific machine becomes a non-trivial problem due to the massive machines in the network that make the connection list too long to identify the target machine. Some solutions such as QR code scanning and proximity estimation have been proposed to solve this problem. However, they have limited performance in scalability and accuracy correspondingly, and thus cannot satisfy the requirements in most applications. Observing the fact that the engineers generally interact with the machines in their line-of-sight, we propose the LightCon scheme which adopts proximity estimation to estimate the machines in the line-of-sight, and controls the display module of machines to show different visible symbols (colors or numbers). To connect with a specific machine, the engineers just need to select the corresponding symbol on the mobile device. Therefore, they do not have to remember the trivial address of each machine. Furthermore, the symbol assignment algorithm is designed to reduce the complexity of manual symbol selection, and its performance is analyzed theoretically. The performance of LightCon is evaluated in the testbed, and the experimental results prove that LightCon is a promising solution to simplify line-of-sight connections with low complexity.

INDEX TERMS Line-of-sight connection, proximity estimation, visible symbols, mobile industrial human machine interaction, industrial Internet of Things.

I. INTRODUCTION

The mobile industrial human-machine interaction (HMI) plays an important role in the industrial internet of things [1]–[4]. With the support of WiFi or Bluetooth [5]–[7], the engineer can interact with the machine at a safe distance by using a mobile device. Moreover, the efficiency of field works can be greatly improved, because the engineer can control the machine and observe its operation simultaneously.

In the mobile industrial HMI, the engineer should connect to the target machine at first by entering its address or selecting it from a list. However, the machines are densely deployed in the industrial plant. Take the power distribution room of the electrical substation shown in Fig.1 as an example, there are 36-48 switch cabinets installed in a room with

The associate editor coordinating the review of this manuscript and approving it for publication was Huan Zhou.

FIGURE 1. Line-of-sight human machine interaction in the power distribution room of the electrical substation.

less than $100m^2$. Due to the broadcasting nature of wireless communication, almost every machine can be scanned by the mobile device that makes the connection list too long to identify the target machine clearly. Since the engineers in the industrial field have to make different connection at 5-20 times per hour, this problem becomes non-trivial that impacts the experience of HMI or even leads to misoperation.

A straightforward solution for this problem is using QR code [8] or NFC [9] that can be scanned to obtain the ID of the machine. However, they should be executed in a short range ($<10cm$) that is not suitable to the scenario that has dangerous or large machines.

Another solution is proximity estimation [10]–[12] which estimates whether nodes are closer than a proximity distance. The application of proximity estimation in the industrial HMI has been discussed in [10], and the FaceME algorithm has been proposed to estimate the machine that is closest to the engineer. However, due to the randomness of wireless signals, FaceME can hardly estimate the closest machine in the plant with dense deployed machines. Besides, the engineers always need to interact with the machine located in their line-of-sight rather than the closest one. In this case, the FaceME can not satisfy its demand.

In this paper, we propose a scheme called *LightCon* to simplify the line-of-sight connection in the mobile industrial HMI. The LightCon uses proximity estimation to estimate the machines located in the line-of-sight, and then controls the display module (LED light or LCD screen) of machines to display different visible *symbols*, such as colors and numbers. In LightCon, the address selection is transferred to the symbol selection, and the list for manual connection is greatly shorten.

LightCon reduces the burden of identifying the target from massive nodes in the scenario with densely-deployed machines. With the help of visible symbols, it can be used to connect with not only the closest machine, but also any machine located in the line-of-sight of the engineer. Moreover, LightCon has low complexity which is helpful to reduce the time delay and the deployment cost.

Specifically, the major contributions of this paper are summarized as follows:

1) A mobile industrial HMI testbed is built to study the challenges in the industrial HMI. The user study and experimental results show that the manual connection to the target machine is non-trivial for the engineer, and the existing algorithm can not satisfy the demand.

2) The LightCon scheme is proposed to simplify line-of-sight connections. In LightCon, the proximity estimation is firstly used to estimate the machines located in the line-of-sight. Then the visible symbols are assigned to the machines according to the estimation results. They will be showed by the display module of machines, and it is helpful for the engineer to identify the target machine.

3) Since multiple rounds of symbol selection may be required when the machines are more than the symbols, we propose two symbol assignment algorithms to reduce the complexity of symbol selection. Then we provide theoretical analysis to study their efficiency.

4) The LightCon is implemented on the testbed to evaluate its performance. Experimental results prove that LightCon is a promising solution to simplify line-of-sight connections with low complexity.

The rest of this paper is briefly introduced as follows. In Section II, the related works of this paper are briefly introduced. Section III introduces the definitions and the testbed used in this paper, and then Section IV evaluates the problems that motivate our works by experiments. Section V provides the details of LightCon scheme and its implementation. Based on LigtCon, the symbol assignment algorithms are proposed in Section VI, and their performance are formally analyzed in Section VII. In Section VIII, the performance of LightCon is evaluated by experiments. Finally, the conclusion is given in Section IX.

II. RELATED WORKS

The interaction and communication between human and machines become more and more important in the industrial internet of things [31], [32]. Supported by wireless technologies such as Bluetooth, the engineer is able to send control commands and read data at any position around the machine. However, the machines are densely deployed in the plant (Fig.1). Due to the broadcasting nature of wireless communication, large number of machines can be scanned by the mobile device that makes the connection list too long to identify the target machine clearly. It is an important problem that impacts the experience of HMI and even leads to misoperation.

QR code [8], [15] or NFC [9], [16] scanning is a straightforward solution which can simplify the data connection by obtaining the ID of machines before connection. However, both of them are not suitable to the scenario with dangerous or large machines due to the extremely short scanning range ($<10cm$). Passive ultra high frequency (UHF) RFID increases the scanning range to 3-10 meters, and thus becomes a popular solution for indoor localization in recent years [28], [29]. Nevertheless, with the growth of the scanning range, multiple tags can be scanned and it is hard for the engineer to identify the target.

The indoor localization technology [17] can be used to estimate the location of the engineer which can be further used to estimate neighbor machines. In [18], the RSSI

(Received Signal Strength Indicator)-based triangulation is used to provide reasonable localization in the indoor environments. The fingerprints-based methods [19], [20] firstly create the radio map by using fingerprints of WiFi signals, and then use the fingerprints map to estimate the location. Some works [21], [30] aggregate the signals of smart sensors and wireless communication to refine the localization results.

Another potential solution is the proximity estimation algorithms [11], [12], [22]–[24] which use RSSI to estimate whether nodes are closer than a proximity distance. The iBeacon developed by Apple is a typical application of proximity estimation, and some algorithms are developed based on iBeacon to improve its estimation accuracy [24], [25]. The paper [11] discussed the face-to-face proximity estimation in the social networks. Combining the data smoothing with the predefined proximity threshold, this work improves the estimation accuracy to 1-1.5m that fulfills the demand of measuring face-to-face proximity.

Most indoor localization and proximity estimation algorithms consider their applications in living buildings which are different from the industrial environments. Take the power distribution room for example, there are 36-48 switch cabinets installed in a room with less than $100m^2$. The node density is much higher than WiFi access points in the living buildings. Our previous works [10], [26], [27] have studied the characteristics and challenges in the wireless industrial HMI, and find that most related works can not provide reasonable estimation accuracy and latency in the industrial HMI due to the dense deployment of machines. On the other hand, we observe that the engineer has to face to the machine during industrial HMI, which makes the relative position between human and machine more useful than the absolute position of engineer.

To overcome these challenges, we have proposed the FaceME algorithm [10] to realize the face-to-machine proximity estimation. In FaceME, the RSSI difference is proposed to estimate the proximal node based on the maximum RSSI, and two-steps estimation is designed to reduce the time complexity. Based on the results that FaceME can hardly estimate the closest machine in the plant, our conference paper [27] provides a preliminary study on how to use visible symbols to simplify the line-of-sight connection. This paper is extended from [27] with improved scheme design, new theoretical and experimental analysis and so on.

Compared with related works, this paper distinguishes them in the following aspects: 1) Visible symbols are used in LightCon to transfer address selection into symbol selection. 2) The visible symbols are assigned dynamically by wireless communication according to the current location of the engineer. 3) The proximity estimation algorithm is used to reduce the nodes involved in symbol assignment. 4) The complexity of line-of-sight connections are analyzed in details with theoretical and experimental studies.

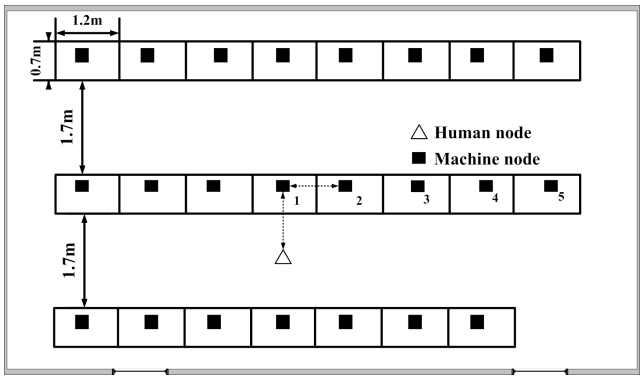

FIGURE 2. The layout of the mobile industrial HMI testbed.

III. PRELIMINARIES

To clarify the description, we firstly provide the definitions used in this paper. Then the mobile industrial HMI testbed used for experiments is introduced.

A. DEFINITIONS

At first, we provide the formal definitions to describe the mobile industrial HMI considered in this paper:

1) The *machine node* is a wireless node connects to each machine in the industrial plant. It is composed of a wireless communication module and a display module (such as LED light) that can display different *visible symbols* such as color or number. We use S to denote the kinds of symbols.

2) The *human node* is a mobile device carried by the engineer. It is the interface for industrial HMI, and it can communicate with machine nodes by wireless communication.

3) The machine node in *line-of-sight* of the engineer should satisfy the following conditions: a) the visible symbol of the node can be clearly identified by the engineer; b) the engineer has the demand to interact with the machine at the current location.

4) The *neighbor list* includes the machine nodes that can be scanned by the human node. The neighbor list is assumed to include every machine node in line-of-sight of the engineer. We use N to denote the number of nodes in the neighbor list.

B. MOBILE INDUSTRIAL HMI TESTBED

We have implemented a mobile industrial HMI testbed in the Delta PLC (Programmable Logic Controller) laboratory [10]. Fig. 2 shows the layout of the testbed. There are 23 control consoles deployed in three rows. The size of the console is 1.2m $\times$ 0.7m, and the width of the passage is 1.7m. The laboratory represents a typical industrial plant where the engineers move in the passage to interact with machines that are densely and regularly deployed [33].

Fig.3 shows the framework of mobile industrial testbed. The testbed contains three parts: the mobile device carried by the engineer is defined as *the human node*, which can connect to machine by bluetooth and display its HMI information. The wireless communication module integrated Bluetooth and RS485 chips is denoted as *the machine node*. And the PLC is designed to control the industrial machine.

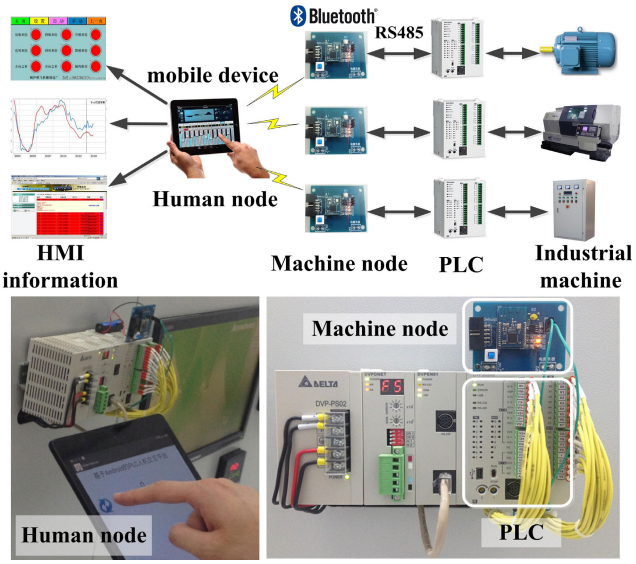

FIGURE 3. The framework of the mobile industrial HMI testbed.

Specifically, 1) Google Nexus 9 is used as the human node, and an Android application is developed to realize industrial human-machine interaction. The FaceME [10] and LightCon are also implemented in the application for analysis.

2) The machine node is composed of an extension board and a core board. The TI-CC2541 chip is embedded in core board for control and Bluetooth communication, and the extension board uses a MAX3485 chip to communicate with machines by RS485 communication. Moreover, three LED lights are used in the extension board to display visible symbols (red, yellow and green).

We will use the testbed to verify the problems in Section IV, and study the performance of LightCon in Section VIII.

IV. PROBLEM STATEMENT

In this paper, we argue that the large number of machine nodes in the industrial internet of things becomes a non-trivial problem for the engineers who have to interact with them in the industrial field. We focus on the connection problem where the engineer has to identify the target machine from the connection list with large number of nodes.

In this section, we firstly study how the length of the connection list impacts the complexity of manual connection. Then the performance of proximity estimation is studied to prove that the existing works is not sufficient to solve the problem.

A. COMPLEXITY OF MANUAL CONNECTION

At first, we study the complexity of manual connection with different length of the connection list. A test Android App is developed to obtain the experimental results. In this App, the user has to touch the start button on the screen, then a node list is displayed on the screen. The target node is randomly generated, and its ID is displayed on the top of the list. Then the user has to select the corresponding ID from the node list and finally clicks the connect button. The selection time is recorded as the duration from the time that the user touches the start button to the time that the connect button is clicked.

TABLE 1. Time of manual connection with different number of nodes in the connection list.

Number of nodes	Selection Time (ms)
3	2158
5	2713
7	3176
10	3956
15	4892
20	5961

TABLE 2. Results of the questionnaire for the preferred number of nodes in the connection list.

Number of nodes	Number of People
0	58 (29.44%)
$[1, 3]$	25 (12.69%)
$[4, 5]$	47 (23.86%)
$[6, 7]$	32 (16.24%)
$[8, 10]$	21 (10.66%)
$[11, 15]$	14 (7.11%)

We invite 197 volunteers to execute this experiment. All the volunteers are the undergraduate or graduate students in the school of electrical engineering and automation at Fuzhou University. The volunteers have to select node ID for 6 times with different length of the list. The length of the list varies from 3 to 20, and the average time of manual connection are given in Table 1. It is clear to see that the manual connection time increases with the growth of the list. When the number of nodes in the list is larger than 20, the selection time grows nearly 6 seconds. Moreover, there are 52 wrong selections appear in the experiments.

After the manual connection experiment, every volunteer has to answer a questionnaire with one simple question: how many nodes do you prefer in the connection list. The statistic results are given in Table 2. There are 130 volunteers (65.99%) that prefer to have less than 5 nodes in the connection list. Moreover, 58 volunteers (29.44%) hope to replace manual connection with automatic connection (0 node in the connection list).

Moreover, we execute an experiment to prove that the connection list with more than 20 nodes is practical in the industrial internet of things. We deploy 23 machine nodes in the Delta PLC laboratory described in Section III-B, and then use the human node to scan machine nodes at the corners of the laboratory. The results show that all 23 machine nodes can be scanned by the human node due to the broadcasting nature of wireless communication. This problem will be more severe if the industrial plant is larger and the range of wireless communication is longer.

To sum up, with the massive nodes in the industrial internet of things, the complexity of manual connection become a non-trivial problem which may results in the waste of time, wrong node selection and the impatience of users.

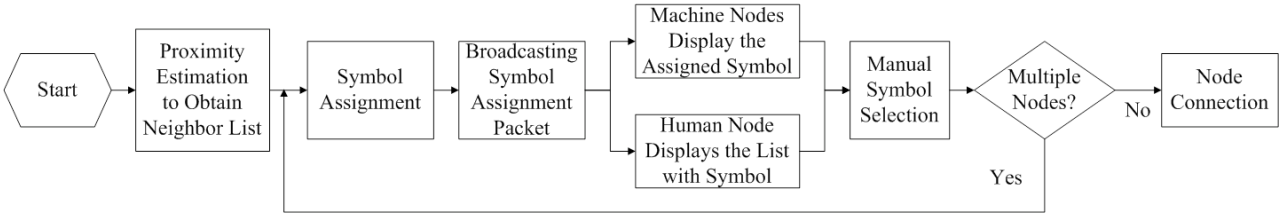

FIGURE 4. The flowchart of LightCon scheme.

TABLE 3. The number of nodes in the estimation results (FaceME).

dy \ dx	1.2	0.6
1.5	1 : 28%	
	2 : 23%	2 : 5%
	3 : 49%	3 : 55%
		4 : 16%
		5 : 24%

B. ACCURACY OF PROXIMITY ESTIMATION

To simplify the node connection, the FaceME algorithm [10] has been proposed to estimate the machine that is closest to the engineers. However, due to the randomness of wireless signals, FaceME can hardly estimate the closest machine in the plant with dense deployed machines.

To verify this problem, we implement the FaceME algorithm in the testbed shown in Fig. 2. There are 23 machine nodes deployed in the testbed, and the human node executes FaceME algorithm to estimate the closest machine node. The node deployment can be formulated by dy which denotes the distance between the human node and the proximal machine node, and dx which denotes the space between machine nodes. In this experiment, the dy is fixed at $1.5m$, and the dx is set as $1.2m$ and $0.6m$ to represent difference machine nodes deployment. The experiment runs 100 times to obtain the statistic results.

The experiment result is given in Table 3. In the table, the integral number indicates the number of nodes in the estimation result, and the percentage that follows each number demonstrates the frequency that the number appears in the experiments. When $dx = 1.2m$, there are 72 times that the estimation results have more than one node. The problem becomes severe when the dx is reduced to $0.6m$. It is 100% that the estimation results have more than one node, and the maximum number of nodes is up to 5.

The multiple nodes in estimation results indicate that the manual connection is required to connect with the target machine. Although the FaceME has greatly reduced the number of nodes in the list (from 23 to 5), it is still a burden for the engineer to identify the ID of the target machine. Moreover, the engineer may need to interact with a machine located in line-of-sight rather than the closest one. In this case, the FaceME can not satisfy the demand.

To solve this problem, we observe that the interaction between the human and machines are always in line-of-sight [31], [32]. Based on this observation, we propose to take advantages of the visible symbol (such as a LED light or screen) which is widely installed on a machine. Then the machine ID selection can be transformed into the symbol selection, and the complexity of data connection to a specific machine is greatly reduced. Based on this idea, a new algorithm called LightCon is proposed in the next section.

V. LIGHTCON SCHEME

LightCon adopts proximity estimation to reduce the number of nodes involved in the manual connection, and then controls the display module of machine nodes to display visible symbols based on symbol assignment algorithm. In this case, the address selection can be transferred to the symbol selection which reduces the burden of identifying the target from massive nodes in the list. The flowchart of LightCon scheme is depicted in Fig. 4.

A. PROXIMITY ESTIMATION

In this paper, LightCon adopts the modified FaceME [10] algorithm for proximity estimation. The RSSI difference is measured in the offline measurement, then the RSSI difference and the maximum RSSI are used in the online estimation to estimate the nodes in line-of-sight. The RSSI value of machine node i is defined as $R(i)$. Due to the fluctuation of the wireless signals, the range of $R(i)$ can be defined as,

$$R(i) \in [L(R(i)), U(R(i))] \tag{1}$$

where $L(R(i))$ is the lower bound of $R(i)$, and $U(R(i))$ is the upper bound of $R(i)$.

Different from FaceME, LightCon changes the definition of RSSI difference to estimate the nodes in line-of-sight rather than the proximal node. Given the set of nodes located in the engineer's line-of-sight C, and the set M^- of all machine nodes except the nodes in C, the definition of RSSI difference is formulated as,

$$\Delta R(C, M^-) = L(R(C)) - U(R(M^-)) \tag{2}$$

where $L(R(C))$ denotes the lower bound of the RSSI of nodes in C, and $U(R(M^-))$ denotes the upper bound of the RSSI of nodes in M^-. The RSSI difference $R(C, M^-)$ reflects the difference between the minimum RSSI of nodes in C and the maximum RSSI of nodes in M^-.

In the offline measurement, the $L(R(C))$ and $U(R(M^-))$ should be measured by the massive RSSI data collection. Specifically, $L(R_1(C))$ and $U(R_1(M^-))$ is defined as the

result calculated by the original data, and $L(R_m(C))$ and $U(R_m(M^-))$ is defined as the result processed by Gaussian filtering algorithm.

The online estimation includes two parts: the preliminary and advanced estimation. In the preliminary estimation, the human node collects the RSSI of each machine node that can be scanned once. Based on that data, the maximum RSSI value $R_{\max}(1)$ of all machine nodes can be obtained. Then, combining the $R_{\max}(1)$ and the $L(R_1(C))$ and $U(R_1(M^-))$ that are measured in offline measurement, the human node can obtain the candidates list called CA.

In the advanced estimation, the human node should further collect the RSSI of machine nodes in the CA for m times. Smoothing the above data by Gaussian filter, the human node can obtain the maximum filtered RSSI value $R_{\max}(m)$. Based on the $R_{\max}(m)$ and the $L(R_m(C))$ and $U(R_m(M^-))$ that are measured in offline measurement, the human node can remove redundant nodes from the CA list to refine the estimation result and obtain the final neighbor list.

B. VISIBLE SYMBOL ASSIGNMENT

When obtains the neighbor list after running proximity estimation algorithm, the human node firstly executes a symbol assignment algorithm to assign symbols for machine nodes. When nodes are more than visible symbols, multiple rounds of symbol selection may be required which directly impacts the complexity of LightCon. Therefore, the symbol assignment algorithms will be discussed in details in Section VI.

When the symbol assignment is completed, the human node generates a SA (symbol assignment) packet that contains the ID and assigned symbols of every node in the neighbor list. Then the SA packet is broadcast by the human node. When the machine node receives the SA packet which contains its ID, it will control the display module to display the assigned symbol.

Meanwhile, after delivering the SA packet, the human node displays a list of visible symbols. The symbols are ordered according to the RSSI values of the nodes assigned to each symbol. After this step, the visible symbols are displayed synchronously on both the machine nodes and the human node.

The engineer checks the visible symbol on the target machine, and then manually selects the same symbol on the human node. Once the symbol is selected, the human node checks the number of nodes that are assigned to the selected symbol, which is denoted as n_k. If $n_k > 1$, the symbol assignment algorithm will be executed again to assign symbols for the rest n_k nodes. The process repeats until $n_k = 1$ is satisfied, then the human node will connect to the machine node left in the list.

C. IMPLEMENTATION

We implement LightCon in the testbed (refer to Section III-B for details) to demonstrate how it works. The human node (Nexus 9) uses Bluetooth to broadcast the SA packet, and the machine node controls its LED light according to the received SA packet. Fig. 5 shows a demonstration with three machine nodes displayed with different symbols (red, yellow and green).

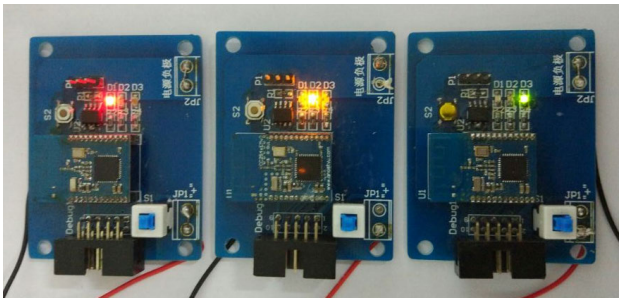

FIGURE 5. Machine nodes with different symbols (colors).

FIGURE 6. The user interface of symbol selection in LightCon.

On the other hand, the human node transforms the neighbors list to the symbols list, and then displays the symbols list on the user interface for manual connection. Fig. 6 demonstrates the user interface that displays the symbols list. The engineer can connect to the target machine by selecting the corresponding color on the list.

Since the number of visible symbols are much less than the number of machines, based on the results given in Section IV-A, the LightCon can greatly reduces the complexity of manual connection in the scenarios with dense deployed machines. Moreover, compared with the number printed on the label, the visible symbol (especially the color) displayed on the machine node is easier to be identified in a distance. Therefore, LightCon can also be used to connect with the large or dangerous machine.

It is important to note that, the LightCon only requires RSSI value for proximity estimation, which is supported by most wireless communication protocols. Therefore, LightCon can be applied with most wireless communication protocols, such as WiFi, Bluetooth and Zigbee. Moreover, the maximum number of symbols depends on the display module of the machine node. We will study the performance of LightCon with different number of symbols in Section VII and VIII-C.

Since most mobile devices support WiFi and Bluetooth communication, and most machine nodes have the display module, the cost of applying LightCon is low. In sum, LightCon is a scalable and cost efficient solution to simplify line-of-sight connections in the industrial internet of things.

VI. SYMBOL ASSIGNMENT ALGORITHMS

When machine nodes are more than the visibile symbols, multiple machine nodes may share a same symbol, which may lead to multiple rounds of symbol selection until the unique node is selected. In this case, the symbol assign algorithm is critical to the complexity of LightCon.

In this section, two symbol assignment algorithms are proposed: average symbol assignment (A-SA) and biased symbol assignment (B-SA). To clarify the description, we denote the current round of symbol selection as k, and the number of nodes in the kth symbol selection is denoted as n_k. Then we can derive an important parameter K as,

$$K = \left\lceil \log_S N \right\rceil \tag{3}$$

The parameter K is used in the symbol assignment algorithms, and it is equal to the maximum round of symbol selection which will be proved in Section VII.

A. AVERAGE SYMBOL ASSIGNMENT (A-SA)

The Average Symbol Assignment (A-SA) algorithm is designed based on a simple idea: divide n_k nodes into S groups equally. Specifically, n_k nodes are divided into h_k groups which have $\lceil \frac{n_k}{S} \rceil$ machine nodes, and $S - h_k$ groups which have $\lfloor \frac{n_k}{S} \rfloor$ machine nodes. The $\lceil\rceil$ and $\lfloor\rfloor$ represent a smallest integer larger than itself and a largest integer smaller than itself, respectively. Formally,

$$n_k = h_k \cdot \left\lceil \frac{n_k}{S} \right\rceil + (S - h_k) \left\lfloor \frac{n_k}{S} \right\rfloor \tag{4}$$

where h_k is equal to the remainder of $\frac{n_k}{S}$,

$$h_k = n_k - S \cdot \left(\left\lceil \frac{n_k}{S} \right\rceil - 1 \right) \tag{5}$$

B. BIASED SYMBOL ASSIGNMENT (B-SA)

In Biased Symbol Assignment (B-SA) algorithm, the given n_k nodes are divided into i_k groups with S^{K-k-1} machine nodes, j_k groups that include S^{K-k} machine nodes, and one group with l_k machine nodes. Formally,

$$n_k = i_k \cdot S^{K-k-1} + j_k \cdot S^{K-k} + l_k \tag{6}$$

The value of i_k, j_k and l_k should satisfy the following constraints,

$$i_k + j_k + 1 = S \tag{7}$$

$$S^{K-k-1} \le l_k < S^{K-k} \tag{8}$$

then we have,

$$i_k = S - \left\lfloor \frac{n_k - S^{K-k-1}}{S^{K-k} - S^{K-k-1}} \right\rfloor \tag{9}$$

$$j_k = \left\lfloor \frac{n_k - S^{K-k-1}}{S^{K-k} - S^{K-k-1}} \right\rfloor - 1 \tag{10}$$

$$l_k = n_k - (j_k + 1) \cdot S^{K-k} + (j_k + 1) \cdot S^{K-k-1} \tag{11}$$

The expression of j_k (10) is derived as follows. Combining (8) and (11), we have,

$$S^{K-k-1} \le n_k - (j_k+1) \cdot S^{K-k} + (j_k+1) \cdot S^{K-k-1} < S^{K-k} \tag{12}$$

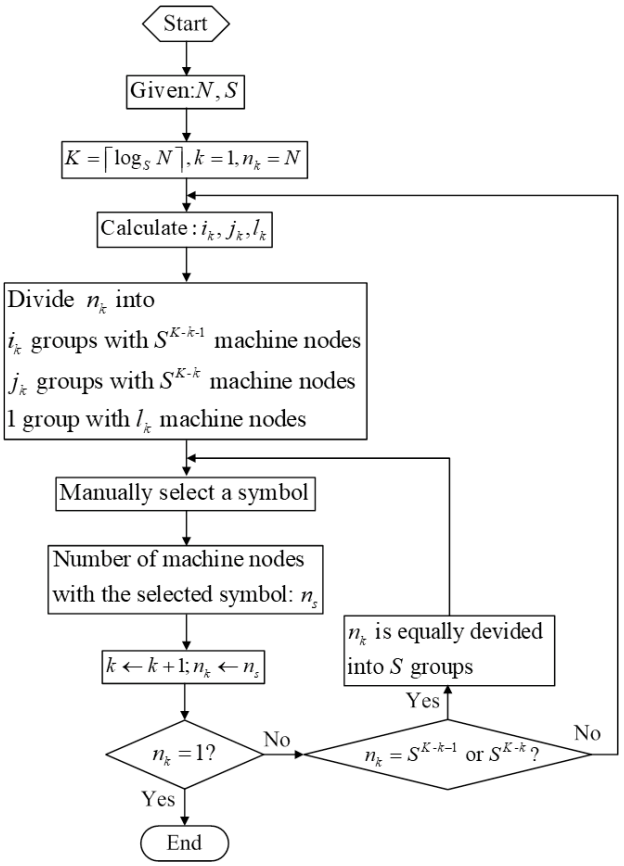

FIGURE 7. Process of Biased Symbol Assignment(B-SA).

Then the range of j_k can be obtained as,

$$\frac{n_k - S^{K-k}}{S^{K-k} - S^{K-k-1}} < j_k + 1 \le \frac{n_k - S^{K-k-1}}{S^{K-k} - S^{K-k-1}} \tag{13}$$

and,

$$\frac{n_k - S^{K-k-1}}{S^{K-k} - S^{K-k-1}} - 2 < j_k \le \frac{n_k - S^{K-k-1}}{S^{K-k} - S^{K-k-1}} - 1 \tag{14}$$

Since j_k is an integer, The (10) can be derived directly based on (14).

The process of B-SA algorithm is shown in Fig. 7. The motivation of designing B-SA algorithm is taking advantage of all the symbols S to minimize the number of nodes involved in the Kth round of symbol selection.

C. CASE STUDY

To clarify the basic idea of the symbol assignment algorithms, we study a case with three different visible symbols ($S = 3$) and five nodes in the neighbor list ($N = 5$). We can derive $K = 2$ based on (3), which means the maximum round of symbol selection is 2.

In this case, the A-SA algorithm divides machine nodes into three groups as {2, 2, 1}. Only one machine node can be connected in one round of symbol selection. The connection to other machines requires two rounds of symbol selection.

The B-SA algorithm divides machine node as {3, 1, 1}. Two nodes can be connected in one round of symbol

TABLE 4. Variables list.

Variable	Description
N	The number of nodes in the neighbor list
S	The number of symbols
K	The maximum round of symbol selection in LightCon
k	The index of current round in symbol selection
n_k	The number of nodes in the kth symbol selection
γ	The rounds of symbol selection required for selecting the target machine node
P	The number of nodes with $\gamma = K - 1$

selection, and the others requires two rounds of symbol selection. B-SA reduces the average round of symbol selection by comparing with A-SA. Their performance will be further analyzed in Section VII and VIII-C.

VII. THEORETICAL ANALYSIS

In LightCon, multiple rounds of symbol selection may be required when the nodes is more than the symbols. The user experience is greatly affected by the rounds of symbol selection, which is denoted by γ. Thus, it is used as the performance metric in this section. The variables used in the analysis are summarized in Table 4.

According to the K defined in (3), the minimum and maximum round of symbol selection are firstly analyzed as follows.

Theorem 1: In A-SA and B-SA algorithms, given N machine nodes and S symbols, for connecting to any machine node, the maximum round of symbol selection is K, and the minimum round of symbol selection is $K - 1$.

Proof 1 (Proof of Theorem 1): In A-SA, at the first round of symbol assignment,

$$N = h_1 \cdot \left\lceil \frac{N}{S} \right\rceil + (S - h_1) \left\lfloor \frac{N}{S} \right\rfloor \tag{15}$$

According to (3), we have,

$$\log_S{}^{\frac{N}{S}} \leq K - 1 < \log_S{}^{N} \tag{16}$$

then,

$$S^{K-2} < \frac{N}{S} \leq S^{K-1} \tag{17}$$

Finally, we deduce that,

$$S^{K-2} < \left\lceil \frac{N}{S} \right\rceil \leq S^{K-1} \tag{18}$$

$$S^{K-2} \leq \left\lfloor \frac{N}{S} \right\rfloor \leq S^{K-1} \tag{19}$$

Combining (18) and (19) with (15), for connecting to any machine node by A-SA algorithm, the rounds of symbol selection is either $K - 1$ or K.

In B-SA, at the first round of symbol assignment,

$$N = i_1 \cdot S^{K-2} + j_1 \cdot S^{K-1} + l_1 \tag{20}$$

For the node in groups with S^{K-2} or S^{K-1} nodes, it is required to execute $K - 1$ or K rounds of symbol selection respectively to establish the connection. For the node in the group with l_1 nodes, since $S^{K-2} < l_1 < S^{K-1}$ (according to (8)), the rounds of symbol selection is either $K - 1$ or K. The proof is completed.

Then we derive the expected rounds of symbol selection. The probability that a machine node is selected as the target is assumed to follow uniform distribution, and the number of nodes with $\gamma = K - 1$ is denoted as P.

Theorem 2: In A-SA algorithm, given N machine nodes and S symbols, the expected rounds of symbol selection is,

$$E_A(\gamma) = \begin{cases} K + 1 - \dfrac{2 \cdot S^{K-1}}{N}, & N \in [S^{K-1}, 2 \cdot S^{K-1}] \\ K, & N \in \left(2 \cdot S^{K-1}, S^K\right] \end{cases} \tag{21}$$

Proof 2 (Proof of Theorem 2): According to Theorem 1, there are P nodes with $\gamma = K - 1$ and $N - P$ nodes with $\gamma = K$, then we can derive,

$$E_A(\gamma) = \frac{P}{N} \cdot (K - 1) + \frac{N - P}{N} \cdot K \tag{22}$$

Since the A-SA algorithm divides nodes into S groups equally, the value of P is determined by the range of N: when $N \in [S^{K-1}, 2 \cdot S^{K-1}]$, $P = 2 \cdot S^{K-1} - N$; when $N \in (2 \cdot S^{K-1}, S^K]$, $P = 0$.

Combining with (22), we can easily deduce (21). The proof is completed.

Theorem 3: In B-SA algorithm, given N machine nodes and S symbols, the expected rounds of symbol selection is,

$$E_B(\gamma) = K - \frac{\sum_{k=1}^{K-1} (i_k{}' \cdot S^{K-k-1})}{N} \tag{23}$$

where

$$i_k{}' = S - \left\lfloor \frac{n_k{}' - S^{K-k-1}}{S^{K-k} - S^{K-k-1}} \right\rfloor \tag{24}$$

$$n_k{}' = \begin{cases} N, & k = 1 \\ n_{k-1}{}' - \left(S - i_{k-1}{}'\right) \cdot \left(S^{K-k-1} - S^{K-k-2}\right), & k \geq 2 \end{cases} \tag{25}$$

Proof 3 (Proof of Theorem 3): Based on (6) given in Section VI-B, the P in B-SA is only relevant to $i_k \cdot S^{K-k-1}$ and l_k.

An iteration with $n_{k+1} = l_k$ can be used to calculate the number of nodes that have $\gamma = K - 1$ in l_k. Combining $n_{k+1} = l_k$ with (9) and (11), we can derive the definition of $i_k{}'$ (24) and $n_k{}'$ (25).

Then the P can be expressed as,

$$P = \sum_{k=1}^{K-1} (i_k{}' \cdot S^{K-k-1}) \tag{26}$$

Combining with (22),

$$E_B(\gamma) = \frac{\sum_{k=1}^{K-1}(i_k' \cdot S^{K-k-1})}{N} \cdot (K-1) + \frac{N - \sum_{k=1}^{K-1}(i_k' \cdot S^{K-k-1})}{N} \cdot K \quad (27)$$

(23) can be directly derived from (27). The proof is completed.

Finally, we analyze the efficiency and optimality of B-SA algorithm as follows.

Corollary 1: The expected rounds of symbol selection in B-SA algorithm is not larger than that in A-SA algorithm.

Proof 4 (Proof of Corollary 1): We define e as the difference between $E(\gamma)$ of A-SA and B-SA, thus the proof of this corollary can be transformed to prove $e = E_A(\gamma) - E_B(\gamma) \geq 0$.

When $N \in \left(2 \cdot S^{K-1}, S^K\right]$, based on (21) and (23), it is clear to derive that,

$$e = \sum_{k=1}^{K-1}(i_k' \cdot S^{K-k-1}) \geq 0 \quad (28)$$

When $N \in \left[S^{K-1}, 2 \cdot S^{K-1}\right]$, we have,

$$e' = e \cdot N = \sum_{k=1}^{K-1}(i_k' \cdot S^{K-k-1}) + N - 2 \cdot S^{K-1} = \frac{S^K - 1}{S-1} + N - 2 \cdot S^{K-1} - \sum_{k=1}^{K-1}\left\lfloor \frac{n_k' - S^{K-k-1}}{S^{K-k} - S^{K-k-1}} \right\rfloor \cdot S^{K-k-1} \quad (29)$$

Further, when $N \in \left[S^{K-1}, 2 \cdot S^{K-1} - S^{K-2}\right)$, we have $\left\lfloor \frac{n_k' - S^{K-k-1}}{S^{K-k} - S^{K-k-1}} \right\rfloor = 1$, then (29) can be simplified as,

$$e' = \frac{S^K - 1}{S-1} + N - 2 \cdot S^{K-1} - \frac{S^{K-2} - 1}{S-1} = N - S^{K-1} + S^{K-2} \geq 0 \quad (30)$$

When $N \in \left[2 \cdot S^{K-1} - S^{K-2}, 2 \cdot S^{K-1}\right]$, we have $\left\lfloor \frac{n_k' - S^{K-k-1}}{S^{K-k} - S^{K-k-1}} \right\rfloor = 2$, then,

$$e' = \frac{S^K - 1}{S-1} + N - 2 \cdot S^{K-1} - 2 \cdot \frac{S^{K-2} - 1}{S-1} = N + S^{K-2} - S^{K-1} - \frac{S^{K-2} - 1}{S-1} \geq 0 \quad (31)$$

Combining the results given above, we have $e \geq 0$ when $N \in \left[S^{K-1}, 2 \cdot S^{K-1}\right]$. The proof is completed.

Corollary 2: The expected rounds of symbol selection in B-SA algorithm is not larger than that in any other symbol assignment algorithms.

Proof 5 (Proof of Corollary 2): We firstly consider the symbol assignment algorithms which have the following characteristic: the minimum round of symbol selection is $K-1$. Based on the proof of Theorem 3, the number of nodes with $\gamma = K-1$ can not be larger than $\sum_{k=1}^{K-1}(i_k' \cdot S^{K-k-1})$. In this case, with given N nodes, the reduction of nodes with $\gamma = K-1$ leads to the growth of nodes with $\gamma \geq K$ which increases the expected rounds of symbol selection.

Then we consider the algorithms whose minimum round of symbol selection is $K-2$. Compared with B-SA algorithm, if there are m nodes with $\gamma = K-2$, at least $m+1$ nodes will be added in the nodes with $\gamma \geq K$. It also increases the expected rounds of symbol selection. The other algorithms are worse than the algorithms discussed above. The proof is completed.

VIII. EXPERIMENTAL EVALUATION

The experiments are executed in the testbed to evaluate the performance of LightCon. According to the analysis in Section VII, the Biased Symbol Assignment (B-SA) algorithm is used in LightCon to assign symbols. The performance are analyzed by two metrics: the connection time and the rounds of symbol selection. The connection time is defined as the duration from the time that the engineer initiates the connection to the time that the connection is completed. The rounds of symbol selection has been defined in Section VII. The results are discussed in the following sections.

A. CONNECTION TIME OF LIGHTCON

In this section, we study the connection time of LightCon in details with three parts: the time of neighbors scanning, the time of SA packet transmission and the time of manual symbol selection.

In the testbed, eight machine nodes are deployed in a row ($N = 8$), and three different symbols can be displayed on every machine node ($S = 3$). According to Theorem 1, the round of symbol selection can be derived as $K = 2$. We invite 7 volunteers to execute data connection to the proximal machine node with LightCon respectively. The number of machine nodes gradually grows from 1 to 8 in the experiments to study its impact on the connection time. Each experiment repeats 10 times, and the human node record the time automatically. The results are summarized in Table 5.

As shown in Table 5, the time of neighbors scanning increases from 221ms to 760ms with the growth of number of nodes. The reason is the interference caused by the broadcasting of multiple machine nodes. The time of neighbors scanning is short when there is only one machine node. However, more nodes leads to more interference in broadcasting, and thus increases the neighbors scanning time.

The time of SA packet transmission also rises when the number of nodes increases. Nevertheless, the maximum time of SA packet transmission is 21ms, which is much less than other parts. Specifically, when there are more than 3 machine nodes, the transmission time clearly becomes larger. It is because the probability that the human node needs to execute

TABLE 5. The connection time of LightCon with different parts.

Time (ms) \ Number of Nodes	1	2	3	4	5	6	7	8
Neighbors Scanning	221.3	301.5	310.9	423.1	404.2	435.4	661.3	767.8
SA Packet Transmission	10.1	10.3	10.2	15.35	16.40	18.75	18.93	20.45
Manual Symbol Selection (1st round)	1010.2	1132	1120.7	1073.8	1091.4	1071.1	1023.4	1138.8
Manual Symbol Selection (2nd round)	0	0	0	1462.3	1654.6	1467.4	1672.2	1687.4
Total Connection Time	1241.6	1443.8	1441.8	2974.55	3166.6	2992.65	3375.83	3614.45

manual connection twice increases when $N > S$. It results in the dual broadcasting of SA packet and the growth of transmission time.

Table 5 shows the time of manual symbol selection in two rounds separately. The time is generally larger than 1000ms, and the major reason is the relatively slow reaction of human. Moreover, the time for the first round of manual connection has no relation with the number of nodes. It is because LightCon transfers the node selection to the symbol selection, and the number of symbols is fixed at 3. On the other hand, the time for the second round of manual connection is zero when number of nodes from 1 to 3. It is because LightCon runs symbol assignment algorithm only once when $N < S$.

Finally, we examine the total connection time which grows from 1245ms to 3610ms with the increasing number of nodes. The reason is that the total connection time is mainly determined by the time of manual symbol selection and neighbors scanning. Specifically, the total connection time grows sharply when $N \geq 4$, because the second round of manual symbol selection appears. Nevertheless, the total time is still less than 3.6 seconds which is acceptable in most applications.

B. CONNECTION TIME COMPARISON

In this part, we study the time of connecting to nodes in line-of-sight by comparing LightCon with that of FaceME [26], QR code scanning [8] and NFC scanning [9]. There are 23 machine nodes deployed in the testbed shown in Fig.2. We invite 7 volunteers to use the human node to connect with nodes 1-5 (Fig.2) in turns. The original position of the human node is in front of the machine node 1, such that the nodes $1-5$ are in the line-of-sight of the volunteer. Each experiment repeats 10 times, and the average connection time is recorded for comparison.

Fig. 8 shows that, if the target machine node is farther from the original position of the human node, more connection time is required in FaceME, QR code scanning and NFC scanning. The major reason is that these methods should be operated in a position that is close to the target machine. Therefore, the volunteer has to move from the original position to the target position which leads to more connection time. While in LightCon, the connection time grows slightly when the distance to the target machine node increases. The reason is that the LightCon uses visible symbols to support the line-of-sight connection, and the volunteer can connect to

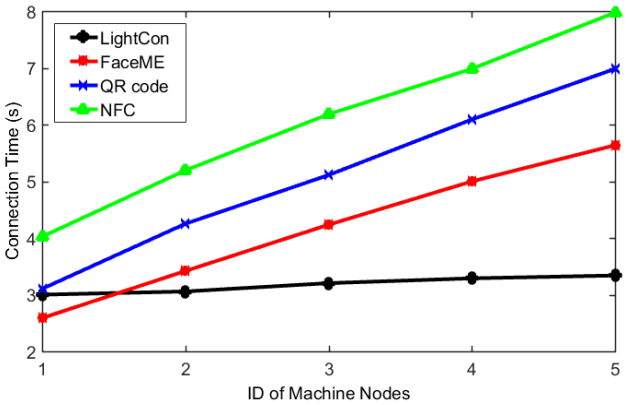

FIGURE 8. Connection time comparison.

the target machine without movement. Nevertheless, according to the observation in the experiments, the volunteers need more time to confirm the visible symbol when the target machine is farther. It results in the slight growth of connection time.

Then we focus on the connection time of machine node 1 which represents the scenario that does not consider the human movement. In this scenario, the connection time of LightCon, QR code scanning, FaceME and NFC scanning are 3s, 3.1s, 2.6s and 4s respectively. NFC scanning has the largest connection time. The major reason is that the human node in the testbed is Nexus 9 which is a 10-inch tablet. The volunteers always have to take several seconds to find the right position to read NFC tags. QR code scanning needs several seconds to open the camera and scan the QR code, while the FaceME spends several seconds to process the RSSI of machine nodes. The connection time of LightCon is slightly larger than that of FaceME, since two rounds of symbol selection is required when the number of nodes in the proximity estimation results is larger than 3.

Based on the results given above, FaceME is a better solution when the engineer only needs to connect with the proximal machine node and the node deployment is sparse enough to estimate the proximal one. In other cases, LightCon performs better than FaceME.

C. ROUNDS OF SYMBOL SELECTION

Finally, we evaluate the performance of A-SA and B-SA algorithms by studying the rounds of symbol selection γ with large number of nodes. We implement both algorithms in

TABLE 6. The rounds of symbol selection γ in A-SA algorithm and B-SA algorithm with different number of machine nodes N and symbols S.

γ S / N	2		3		4		5	
	A-SA	B-SA	A-SA	B-SA	A-SA	B-SA	A-SA	B-SA
5	2:6029 3:3971	2:7549 3:2451	1:2021 2:7979	1:6683 2:3317	1:5978 2:4022	1:7517 2:2483	1:10000 2:0	1:10000 2:0
10	3:6033 4:3967	3:7513 4:2487	2:7953 3:2047	2:8915 3:1085	2:10000 3:0	1:4994 2:5006	2:10000 3:0	1:5486 2:4514
15	3:708 4:9292	3:1226 4:8774	2:1988 3:8012	2:6618 3:3382	2:10000 3:0	2:10000 3:0	2:10000 3:0	1:3223 2:6777
20	4:4011 5:4011	4:7509 5:2491	3:10000 4:0	2:3326 3:6674	2:6039 3:3961	2:8541 3:1459	2:10000 3:0	1:1985 2:8015
25	4:2804 5:7196	4:4360 5:5640	3:10000 4:0	2:1117 3:8883	2:2874 3:7126	2:8117 3:1883	2:10000 3:0	2:10000 3:0
30	4:657 5:9343	4:1226 5:8774	3:7992 4:2008	3:9251 4:0749	2:770 3:9330	2:6663 3:3337	2:6630 3:3370	2:9114 3:886
35	5:8259 6:1741	5:9051 6:949	3:5369 4:4631	3:8510 4:1480	3:10000 4:0	2:5726 3:4274	2:4269 3:5731	2:8613 3:1387
40	5:5996 6:4004	5:7507 6:2493	3:3527 4:6473	3:7382 4:2618	3:10000 4:0	2:5098 3:4902	2:2458 3:7542	2:8328 3:1672

Matlab for simulations, since the testbed can not support the experiments that have large number of machines nodes with different number of symbols.

The number of nodes N varies from 5 to 40, and the number of symbols S grows from 2 to 5. The target machine is randomly selected, and the LightCon scheme with A-SA and B-SA algorithms run separately to connect with the target machine. We calculate the rounds of symbol selection by running 10000 times with every setting of N and S. The results are given in Table 6. In the table, the number before the colon means the value of γ, and the number after the colon presents the times that each γ appears in the experiments.

As shown in Table 6, the rounds of symbol selection is either K or $K-1$ which proves the correctness of Theorem 1. When the number of nodes N increases from 5 to 40, the rounds of symbol selection γ grows with the same number of symbols S. When the number of nodes is larger than 20 and the number of symbols S is 2, the rounds of symbol selection is larger than 4 which can hardly be tolerated by the users.

Nevertheless, this problem can be solved with more symbols. Given the same number of nodes N, the γ is reduced when the number of symbols increases. When the number of symbols S is larger than 4, no more than 3 rounds of symbol selection is required even if $N = 40$. This result proves that the LightCon can satisfy the demands in most industrial internet of things with densely deployed nodes, and it can work with wireless technologies that have larger transmission range than Bluetooth (such as WiFi and Zigbee).

Finally, we compare the performance of A-SA and B-SA. Table 6 shows that, given the same S and N, the γ in B-SA algorithm is no larger than that in A-SA algorithm. Furthermore, the advantage of B-SA algorithm is larger with more symbols. These results coincide with theoretical analysis given in Section VII.

IX. CONCLUSION

This paper considers the challenges of the line-of-sight connection in the mobile industrial HMI. A testbed is implemented to study the problem, and then the LightCon scheme is proposed to use proximity estimation and visible symbol assignment to simplify line-of-sight connections. The symbol assignment algorithm is designed to reduce the complexity of symbol selection, and its performance is analyzed theoretically. The performance of LightCon is evaluated in the testbed, and the experimental results prove that LightCon is a promising solution to simplify line-of-sight connections with low complexity.

REFERENCES

[1] A. Ajith Kumar S., K. Ovsthus, and L. M. Kristensen, "An industrial perspective on wireless sensor networks—A survey of requirements, protocols, and challenges," *IEEE Commun. Surveys Tuts.*, vol. 16, no. 3, pp. 1391–1412, 3rd Quart., 2014.

[2] C. Chen, J. Yan, N. Lu, Y. Wang, X. Yang, and X. Guan, "Ubiquitous monitoring for industrial cyber-physical systems over relay-assisted wireless sensor networks," *IEEE Trans. Emerg. Topics Comput.*, vol. 3, no. 3, pp. 352–362, Sep. 2015.

[3] Z. Iqbal, K. Kim, and H.-N. Lee, "A cooperative wireless sensor network for indoor industrial monitoring," *IEEE Trans. Ind. Informat.*, vol. 13, no. 2, pp. 482–491, Apr. 2017.

[4] H. Xu, W. Yu, D. Griffith, and N. Golmie, "A survey on industrial Internet of Things: A cyber-physical systems perspective," *IEEE Access*, vol. 6, pp. 78238–78259, 2018.

[5] J. A. Frank and V. Kapila, "Towards natural interfaces to interact with physical systems using smart mobile devices," in *Proc. 40th Annu. Conf. IEEE Ind. Electron. Soc. (IECON)*, Oct./Nov. 2014, pp. 2458–2464.

[6] R. Rondón, M. Gidlund, and K. Landernäs, "Evaluating Bluetooth low energy suitability for time-critical industrial iot applications," *Int. J. Wireless Inf. Netw.*, vol. 24, no. 3, pp. 278–290, Sep. 2017.

[7] L. Leonardi, G. Patti, and L. L. Bello, "Multi-hop real-time communications over Bluetooth low energy industrial wireless mesh networks," *IEEE Access*, vol. 6, pp. 26505–26519, 2018.

[8] H. Zhang, C. Zhang, W. Yang, and C.-Y. Chen, "Localization and navigation using QR code for mobile robot in indoor environment," in *Proc. IEEE Int. Conf. Robot. Biomimetics*, Dec. 2015, pp. 2501–2506.

[9] R. Ramanathan and J. Imtiaz, "NFC in industrial applications for monitoring plant information," in *Proc. Int. Conf. Comput., Commun. Netw. Technol. (ICCCNT)*, Jul. 2013, pp. 1–4.
[10] Z. Xu, R. Wang, X. Yue, T. Liu, C. Chen, and S. Fang, "FaceME: Face-to-machine proximity estimation based on RSSI difference for mobile industrial human–machine interaction," *IEEE Trans. Ind. Informat.*, vol. 14, no. 8, pp. 3547–3558, Aug. 2018.
[11] S. Liu, Y. Jiang, and A. Striegel, "Face-to-face proximity estimationusing Bluetooth on smartphones," *IEEE Trans. Mobile Comput.*, vol. 13, no. 4, pp. 811–823, Apr. 2014.
[12] S. Lakshmipriya and V. Gowthaman, "Improving proximity evaluation for smartphone via bluetooth," *Int. J. Eng. Technol. Sci.*, vol. 2, no. 3, pp. 82–86, 2015.
[13] V. C. Gungor and G. P. Hancke, "Industrial wireless sensor networks: Challenges, design principles, and technical approaches," *IEEE Trans. Ind. Electron.*, vol. 56, no. 10, pp. 4258–4265, Oct. 2009.
[14] F. Barac, S. Caiola, M. Gidlund, E. Sisinni, and T. Zhang, "Channel diagnostics for wireless sensor networks in harsh industrial environments," *IEEE Sensors J.*, vol. 14, no. 11, pp. 3983–3995, Nov. 2014.
[15] M. Nowicki, M. Rostkowska, and P. Skrzypczyński, "Indoor navigation using QR codes and WiFi signals with an implementation on mobile platform," in *Proc. Signal Process., Algorithms, Architectures, Arrangements, Appl. (SPA)*, Sep. 2016, pp. 156–161.
[16] L. Tamazirt, F. Alilat, and N. Agoulmine, "NFC-based ubiquitous monitoring system for e-industry," in *Proc. 3rd Int. Conf. Mobile Secure Services (MobiSecServ)*, Feb. 2017, pp. 1–4.
[17] A. Yassin, Y. Nasser, M. Awad, A. Al-Dubai, R. Liu, C. Yuen, R. Raulefs, and E. Aboutanios, "Recent advances in indoor localization: A survey on theoretical approaches and applications," *IEEE Commun. Surveys Tuts.*, vol. 19, no. 2, pp. 1327–1346, 2nd Quart., 2016.
[18] A. Awad, T. Frunzke, and F. Dressler, "Adaptive distance estimation and localization in WSN using RSSI measures," in *Proc. Eur. Conf. Digit. Syst. Design Architectures, Methods Tools (DSD)*, Aug. 2007, pp. 471–478.
[19] Y. Shu, Y. Huang, J. Zhang, P. Coué, P. Cheng, J. Chen, and K. G. Shin, "Gradient-based fingerprinting for indoor localization and tracking," *IEEE Trans. Ind. Electron.*, vol. 63, no. 4, pp. 2424–2433, Apr. 2016.
[20] X. Tian, W. Li, Y. Yang, Z. Zhang, and X. Wang, "Optimization of fingerprints reporting strategy for WLAN indoor localization," *IEEE Trans. Mobile Comput.*, vol. 17, no. 2, pp. 390–403, Feb. 2018.
[21] Z. Chen, H. Zou, H. Jiang, Q. Zhu, Y. C. Soh, and L. Xie, "Fusion of WiFi, smartphone sensors and landmarks using the Kalman filter for indoor localization," *Sensors*, vol. 15, no. 1, pp. 715–732, Jan. 2015.
[22] C. Chen, S. Zhu, X. Guan, and X. Shen, "Distributed consensus estimation of wireless sensor networks," in *Wireless Sensor Networks*. Cham, Switzerland: Springer, 2014.
[23] J.-Y. Jung, D.-O. Kang, J.-H. Choi, and C.-S. Bae, "D2D distance measurement using Kalman filter algorithm for distance-based service in an office environment," in *Proc. 17th Int. Conf. Adv. Commun. Technol.*, Jul. 2015, pp. 221–224.
[24] F. Zafari, I. Papapanagiotou, M. Devetsikiotis, and T. J. Hacker, "Enhancing the accuracy of iBeacons for indoor proximity-based services," in *Proc. IEEE Int. Conf. Commun. (ICC)*, May 2017, pp. 1–7.
[25] H. Zou, H. Jiang, Y. Luo, J. Zhu, X. Lu, and L. Xie, "BlueDetect: An iBeacon-enabled scheme for accurate and energy-efficient indoor-outdoor detection and seamless location-based service," *Sensors*, vol. 16, no. 2, p. 268, 2016.
[26] T. Liu, Z. Xu, R. Wang, H. Jiang, C. Chen, and S.-H. Fang, "Face-to-machine proximity estimation for mobile industrial human machine interaction," in *Proc. IEEE Int. Conf. Commun. (ICC)*, May 2017, pp. 1–6.
[27] X. Yue, Z. Xu, W. Huang, R. Wang, H. Jiang, C. Chen, and S.-H. Fang, "LightCon: Simplify line-of-sight connection with visible symbols in industrial wireless networks," in *Proc. 43rd Annu. Conf. IEEE Ind. Electron. Soc. (IECON)*, Oct./Nov. 2017, pp. 3480–3485.
[28] J. Zhang, Y. Lyu, J. Patton, S. C. G. Periaswamy, and T. Roppel "BFVP: A probabilistic UHF RFID tag localization algorithm using Bayesian filter and a variable power RFID model," *IEEE Trans. Ind. Electron.*, vol. 65, no. 10, pp. 8250–8259, Oct. 2018.
[29] Y. Zhao, K. Liu, Y. Ma, Z. Gao, Y. Zang, and J. Teng, "Similarity analysis-based indoor localization algorithm with backscatter information of passive UHF RFID tags," *IEEE Sensors J.*, vol. 17, no. 1, pp. 185–193, Jan. 2017.
[30] D. B. Haddad, W. A. Martins, M. D. V. M. da Costa, L. W. P. Biscainho, L. O. Nunes, and B. Lee, "Robust acoustic self-localization of mobile devices," *IEEE Trans. Mobile Comput.*, vol. 15, no. 4, pp. 982–995, Apr. 2016.
[31] D. Gorecky, M. Schmitt, M. Loskyll, and D. Zühlke, "Human-machine-interaction in the industry 4.0 era," in *Proc. 12th IEEE Int. Conf. Ind. Inform. (INDIN)*, Jul. 2014, pp. 289–294.
[32] C. Wittenberg, "Human-CPS interaction—Requirements and human-machine interaction methods for the industry 4.0," *IFAC-PapersOnLine*, vol. 49, no. 19, pp. 420–425, 2016.
[33] H. Hosseini-Nasab, S. Fereidouni, S. M. T. F. Ghomi, and M. B. Fakhrzad, "Classification of facility layout problems: A review study," *Int. J. Adv. Manuf. Technol.*, vol. 94, nos. 1–4, pp. 957–977, 2018.

ZHEZHUANG XU (S'10–M'14) received the B.Eng. degree in automation from Xiamen University, Xiamen, China, in 2005, the M.Eng. degree in measuring and testing technologies and instruments from Jiangsu University, Zhenjiang, China, in 2008, and the Ph.D. degree in control science and engineering from Shanghai Jiao Tong University, Shanghai, China, in 2012.

He joined the School of Electrical Engineering and Automation, Fuzhou University, Fuzhou, China, in 2012, where he is currently an Associate Professor. He is the Director of the Public Platform of Industrial Big Data Application, Fujian Provincial Commission of Economy and Information Technology. He has authored and coauthored over 30 refereed international journal and conference papers. His research interests include wireless communication and big data analysis in the industrial Internet of Things.

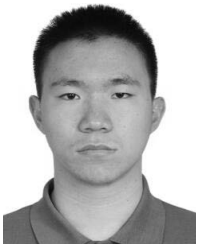

ANGUO LIU is currently pursuing the bachelor's degree with the School of Electrical Engineering and Automation, Fuzhou University, Fuzhou, China.

He has authored one article accepted in the 31st Chinese Control and Decision Conference (CCDC 2019). His research interest includes digital control technology and its application in the industrial Internet of Things.

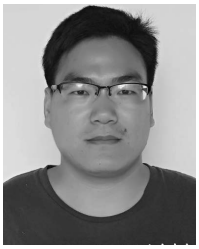

XI YUE received the B.Eng. degree in electrical engineering from the Yangtze University of China, Jingzhou, China, in 2014, and the master's degree in control theory and control engineering from Fuzhou University, Fuzhou, China, in 2018.

He is currently a Designer with the Institute of Space Science and Technology, XiaoGan, China. His research interests include testbed design and big data analysis in the industrial Internet of Things. He has authored one article in the 43rd Annual Conference of the IEEE Industrial Electronics Society (IECON 2017).

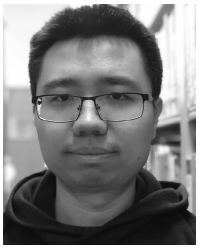

YULONG ZHANG is currently pursuing the bachelor's degree with the School of Electrical Engineering and Automation, Fuzhou University, Fuzhou, China.

His research interest includes proximity estimation algorithms design and its application in the mobile industrial human–machine interaction. He has authored one article accepted in the 3rd International Symposium on Autonomous Systems (ISAS-2019).

RONGKAI WANG (S'18) received the B.Eng. degree in electrical engineering and automation from Hangzhou Dianzi University, Hangzhou, China, in 2016, and the master's degree in control theory and control engineering with Fuzhou University, Fuzhou, China, in 2019. He is currently pursuing the D.Eng. degree in electronic and information with Zhejiang University, Hangzhou.

His current research interests include proximity estimation algorithms design, and wireless signal processing and their applications in the mobile industrial human–machine interaction. He has authored one article in the IEEE TRANSACTIONS ON INDUSTRIAL INFORMATICS, and one article in the 1st IEEE International Conference on Industrial Cyber-Physical Systems (ICPS-2018).

JIE HUANG (M'15) received the B.E. degree in electrical engineering and automation, and the M.E. degree in control engineering from Fuzhou University, China, in 2005 and 2010, respectively, and the Ph.D. degree in control science and engineering from the Beijing Institute of Technology, Beijing, China, in 2015.

From 2014 to 2018, he held postdoctoral and lecturer appointments with the Faculty of Science and Engineering, University of Groningen, The Netherlands. He is currently a Professor with the School of Electrical Engineering and Automation, Fuzhou University, China. He is the Vice-President of the Fujian Automation Association, Fujian, China. His research interests include human–robot cooperation and multi-agent systems.

SHIH-HAU FANG (M'09–SM'13) is currently a Full Professor with the Department of Electrical Engineering, Yuan Ze University (YZU), and the MOST Joint Research Center for AI Technology and All Vista Healthcare, Taiwan. He was a Software Architect with Chung-Hwa Telecom Company Ltd., from 2001 to 2007, and joined YZU, in 2009. His research interests include indoor positioning, mobile computing, machine learning, and signal processing.

Prof. Fang received the YZU Young Scholar Research Award, in 2012 and the Project for Excellent Junior Research Investigators, Ministry of Science and Technology, in 2013. His team won the third place of the IEEE BigMM HTC Challenge, in 2016, and the third place of IPIN, in 2017. He is currently the Technical Advisor of HyXen Technology Company Ltd., and serves as an Associate Editor for the *IEICE Transactions on Information and Systems*.